

Unclassified

SECURITY CLASSIFICATION OF THIS PAGE (When Data Entered)

REPORT DOCUMENTATION PAGE		READ INSTRUCTIONS BEFORE COMPLETING FORM
1. REPORT NUMBER PSSL-160676	2. GOVT ACCESSION NO.	3. RECIPIENT'S CATALOG NUMBER
4. TITLE (and Subtitle) The Stability of Dielectric Coatings under Radiation,	5. TYPE OF REPORT & PERIOD COVERED Final 1 October 1974 31 March 1976	6. PERFORMING ORG. REPORT NUMBER 1288-AMS
7. AUTHOR(s) B.S.H. Royce S. T. Wang	8. PERFORMING ORG. REPORT NUMBER N00014-75-C-1022	9. PROGRAM ELEMENT, PROJECT, TASK AREA & WORK UNIT NUMBERS DNA Subtask 299Q AXTA 007 Work Unit 52
10. CONTROLLING OFFICE NAME AND ADDRESS Office of Naval Research Arlington, Virginia 22217	11. REPORT DATE 31 March 1976	12. NUMBER OF PAGES 29
13. MONITORING AGENCY NAME & ADDRESS (if different from Controlling Office) Naval Research Laboratory (Code 5216 HH)	14. SECURITY CLASS. (of this report) Unclassified	15a. DECLASSIFICATION/DOWNGRADING SCHEDULE
16. DISTRIBUTION STATEMENT (of this Report) Approved for Public Release; Distribution Unlimited.		
17. DISTRIBUTION STATEMENT (of the abstract entered in Block 20, if different from Report) ADP07		
18. SUPPLEMENTARY NOTES The findings in this report are not to be construed as an official Office of Naval Research position, unless so designated by other authorized documents.		
19. KEY WORDS (Continue on reverse side if necessary and identify by block number) MOS, Thermal Annealing Radiation Hardness CCD, Ion Implantation Low Temperatures Electron Traps Photodepopulation		
20. ABSTRACT (Continue on reverse side if necessary and identify by block number) Research performed was directed at understanding the effects of ion implantation on the radiation hardness of the SiO <sub>2</sub> gate oxide of MOS devices. MOS capacitors were used as test structures and capacitance-voltage measurements were combined with photo-injection, photodepopulation, thermal annealing and variable temperature measurements on both implanted and unimplanted samples		

DD FORM 1 JAN 73 1473

EDITION OF 1 NOV 65 IS OBSOLETE  
S/N 0102-014-6601

Unclassified  
SECURITY CLASSIFICATION OF THIS PAGE (When Data Entered)

AD A030670

Unclassified

Security Classification of this Page(When Data Entered)

in order that the modified oxide charge trapping could be probed. Some measurements were made using the scanning electron microscope as a source of electrons of controlled energy. C-V and G-V data was taken with the MOS samples in the microscope environment, the beam energy being slowly increased to probe the oxide to increasing depths.

The experimental data indicates that the primary effect of the implantation process is to produce electron traps associated with the implantation induced displacement damage. At room temperature, electrons in these traps can charge compensate holes trapped near the Si/SiO<sub>2</sub> interface. At low temperatures however, the increased hole trapping at this interface overcomes the effects of the trapped electrons and dominates the flat band voltage shifts.

A model of the charge trapping behavior has been developed which satisfactorily explains the observed behavior.



Telecom - Miss. Univ., DNA.  
Proj. No. DNA-NWED-QAXT  
A007-105PM1.  
18 Oct 56 - 246

Unclassified

Security Classification of this Page(When Date Entered)

## THE STABILITY OF DIELECTRIC COATINGS UNDER RADIATION

### I. INTRODUCTION

Metal-Oxide-Semiconducting structures are becoming increasingly important in large scale integrated circuits for data processing and memory uses and in charged coupled devices used as solid state imaging systems. In the ideal system the oxide is an inert insulator separating the metal gate electrode from the semiconducting substrate. In satellite applications, MOS structures are exposed to an ionizing radiation environment and the insulator is no longer a passive element. Electrons and holes are created in the insulator or injected into it from the metal gate electrode and the semiconducting substrate. Some of these carriers become trapped in the oxide, altering the field at the silicon surface and hence the operating threshold of the device. This charge storage can take the threshold out of the range available from the power supplies associated with the circuits or cause power consuming leakage currents. If the device is operated at low temperatures, such as may be desirable in a sensitive infrared solid state imaging system, the trapping of positive charges in the oxide is greatly increased and image deterioration occurs at total doses as low as  $10^4$  rads (Si).

Three approaches have been used in an attempt to improve oxide behavior in a radiation environment:<sup>(1)</sup>

(a) Strict control of the conditions under which the  $\text{SiO}_2$  is grown, including the surface preparation of the Si and freedom from ionic contaminants such as Na.

(b) Modifications of  $\text{SiO}_2$ , produced under the conditions determined in (a), by ion-implantation with Al or the diffusion of chromium into the oxide.

(c) The use of a gate insulator other than  $\text{SiO}_2$ , with  $\text{Al}_2\text{O}_3$  being the favored alternative.

This report is concerned with experiments that have been made on Al implanted,  $\text{SiO}_2$  insulated MOS capacitor structures in order to understand the changes in oxide charge storage produced by the implantation, the thermal

stability of the oxide modifications and their spatial distribution within the oxide. The techniques of photoinjection, photodepopulation, and capacitance-voltage measurements have been used to determine the electronic trap structure of both implanted and unimplanted  $\text{SiO}_2$  and its response to ionizing radiation. The scanning electron microscope has been used as a source of radiation with a controllable penetration into the oxide as well as an imaging system. The results of studies on samples implanted at different energies and of thermal annealing experiments are discussed below and a simple model is presented which explains the observed equilibrium charge storage behavior under both positive and negative gate bias conditions.

The data presented indicates that ion implantation is a suitable technique for controlling the radiation hardness of MOS structures at room temperature. The low temperature data, however, indicates that the compensatory electron traps introduced by the ion implantation process are not able to compensate for the increased interfacial hole trapping that occurs at liquid nitrogen temperatures. Alternate methods are therefore needed to increase the hardness of CCD's used as low temperature imaging devices.

## II. EXPERIMENTAL

In order to determine the effects of implantation and thermal annealing on the electrical behavior of MOS systems, measurements were made on the charge storage in both unimplanted and implanted MOS capacitors as a function of X-ray dose, sample temperature, bias during irradiation and annealing history. The oxides used were grown on  $3\Omega\text{cm}$   $\langle 100 \rangle$  n-type silicon to a thickness of  $1315 \pm 20 \text{ \AA}$  by dry oxidation at Hughes Aircraft<sup>(2)</sup>. The  $\text{Al}^+$  implantation was with  $10^{14}$  or  $10^{15}$  ions  $\text{cm}^{-2}$  at 10, 20 or 30 KeV. On the basis of ion microprobe measurements<sup>(3)</sup> the 20 KeV implantation is known to produce an  $\text{Al}^+$  ion distribution with its peak between 200 and 500  $\text{\AA}$  from the gate electrode. Either semi-transparent gold or opaque aluminum gate electrodes were vacuum evaporated onto the samples. The gold electrodes had a thickness of about 150  $\text{\AA}$  and enabled photodepopulation methods to be used to study the charge trapped after X-irradiation.

For the measurements discussed below each sample was mounted on the cold finger of a vacuum cryostat and could be subjected to various experimental probes. The apparatus has been previously described<sup>(4)</sup>. The sample temperature could be controlled in the range between 80 and 300°K and all measurements could be made at any temperature.

X-irradiation of the sample was performed at 90 KeV, 20mA with a tungsten target tube. The estimated dose rate at the sample was  $10^6$  rads (Si) per hour. Light for the photodepopulation studies came from a Xenon source used in conjunction with wide band filters. The charge state of the capacitor was determined using Capacitance-Voltage (C-V) techniques<sup>(5)</sup> with the flat band voltage condition being used to provide a measure of the charge stored in the oxide and in interface states. A Boonton Model 72B Capacitance meter was used to measure the small signal capacitance at a frequency of 1 MHz in conjunction with a voltage ramp that could be varied between 0.01V/sec and 10V/sec. Thermal annealing was performed in a vacuum furnace of low thermal inertia with the sample held between sapphire plates. The furnace and the plates were specially cleaned to minimize any uptake of sodium during the annealing process. Both isochronal and isothermal annealing measurements were made. Some samples were mounted on the specimen stage of a scanning electron microscope developed at Princeton. The microscope specimen chamber was modified to allow electrical interaction with the specimens and C-V and G-V measurements were made on capacitor samples within the microscope after various exposures to the electron beam. Samples were held under a constant bias of +10 volts with the gate electrode at ground potential. The electron beam current was maintained at  $10^{-8}$  amps and the samples exposed for periods of 15, 30, 60 and 120 seconds at various beam energies between 500 and 4000 eV. The electron beam energy was increased in 100 volt steps after each exposure series and the chosen energy range corresponded to electrons stopping in the gate electrode, the oxide and, at the highest energy, in the silicon substrate. A minicomputer was coupled to the measuring apparatus and used to compute the interface state density after each exposure.

### III. RESULTS

#### a. The Unimplanted Oxide.

Extensive measurements have been made of the behavior of unimplanted oxide samples exposed to ionizing radiation at both room temperature and liquid nitrogen temperature. These results have been previously reported<sup>(6)</sup>. Figure 1 summarizes the saturated flat band voltage behavior of a typical sample exposed to X-rays at either room temperature or liquid nitrogen temperature. The data points were obtained by setting the desired gate voltage and exposing the capacitor to X-irradiation for approximately 3 hours. The saturated flat band voltage shift was then measured, the gate voltage changed to the next value and the radiation exposure continued for a similar time. Each data point therefore represents an additional  $3 \times 10^6$  rads (Si) of irradiation with respect to the previous point. The gate voltage on the specimen was varied in a random way for each run. The saturated flat band voltage,  $V(\text{sat})$ , depends upon the temperature and the bias on the sample during X-irradiation but is independent of the flat band voltage condition at the beginning of an exposure<sup>(7)</sup>.

It is seen that the unimplanted oxide has a net positive charge storage for both gate bias polarities at room temperature and at liquid nitrogen temperature. At liquid nitrogen temperatures the oxide stored less positive charge under negative bias than under the corresponding bias at room temperature. For positive gate voltages up to about 10 volts considerably more positive charge was stored in the oxide at 80°K than at room temperature. Photodepopulation studies indicated that this additional charge was in different traps from those associated with room temperature hole trapping since it could be removed by photons with an energy of circa 2.5 eV, whereas the charge stored in the room temperature stable traps could not be photodepopulated<sup>(6)</sup>. These additional traps are close to the Si/SiO<sub>2</sub> interface and may be emptied by field emission processes.

#### b. The Implanted Oxide

Figure 2 shows the corresponding saturated flat band voltage shift as a function of gate voltage during X-irradiation for the implanted oxide samples.

Under negative bias conditions the charge storage was very similar to that in the unimplanted oxide, with  $V(\text{sat})$  having a linear dependence on  $V_g$  at both 80°K and room temperature and indicating net positive charge storage in the oxide. Under positive gate voltage conditions the behavior at room temperature was quite different from that of the unimplanted oxide.  $V(\text{sat})$  was positive, corresponding to net negative charge storage in the oxide, for X-ray doses of circa  $3 \times 10^6$  rads (Si). The value of  $V(\text{sat})$  under these positive gate voltage conditions was also found to depend upon the energy of  $\text{Al}^+$  implantation. Values obtained under a +10 volt gate bias are given in Table 1, and it is seen that  $V(\text{sat})$  is more positive for the higher implantation energies.

The positive flat band voltage resulting from room temperature X-irradiation could be taken to negative values by prolonged exposure to 4.9 eV light under negative gate voltage conditions (Fig. 3). With this bias, electron injection from the semitransparent gold electrodes is small and most of the injected electrons are expected to be trapped in the displacement damage zone close to that electrode. The effect is therefore thought to be due to the photodepopulation of electrons trapped in the radiation damage zone during the X-ray exposure. This is supported by the observation that, under the same conditions, the flat band voltage of an unimplanted sample always shifts from its initial negative value towards zero.

At liquid nitrogen temperatures there was a net positive charge storage in the implanted oxide under all positive gate bias conditions (Fig. 2). Photodepopulation measurements indicated that this positive charge corresponded to the additional low temperature charge stored in the unimplanted oxide at 80°K, since it could be removed by illuminating the sample with photons of energy less than 2.5 eV. Under photodepopulation conditions at 80°K the flat band voltage shift could be reduced to zero by about 20 mins. illumination and taken to positive values by longer illumination. These measurements clearly indicate that charge compensation processes are involved in the radiation response of an implanted oxide.

#### c. Annealing of Implantation Associated Damage

In order to study the annealing of traps associated with the implanta-

tion of  $\text{Al}^+$  ions into the  $\text{SiO}_2$  matrix and the associated negative charge storage in these oxides, MOS capacitors were annealed in a vacuum ambient for 30 mins. at a series of temperatures between  $100^\circ$  and  $500^\circ$  C. After each anneal the saturated flat band voltage produced by subsequent room temperature X-irradiation was measured for gate biases of +4 and +10 volts. Spot checks were made on  $V(\text{sat})$  obtained under negative bias conditions. Fig. 4 shows the data obtained under positive gate bias. It is seen that the amount of negative charge stored in the oxide decreased as the annealing temperature increased and that  $V(\text{sat})$  changed sign as higher annealing temperatures were reached, the fully annealed oxide storing net positive charge. The temperature at which  $V(\text{sat})$  changed sign was seen to be gate voltage dependent, indicating that it is not just the number of traps but their state of occupancy that is important in determining  $V(\text{sat})$ . If the change in  $V(\text{sat})$  at the 4 volt gate bias produced by an anneal at a given temperature is expressed as a fraction of the corresponding shift measured with a 10 volt gate bias, the fraction is found to be a constant, independent of the anneal temperature, having a value equal to the ratio of the gate biases. This suggests that the reduction of the bulk oxide field to zero by the trapped charges is important in determining the equilibrium trap occupancy and hence  $V(\text{sat})$ .

In addition to these isochronal measurements some samples were annealed isothermally so that activation energies associated with the annealing of the lattice displacement damage could be obtained. Preliminary results indicate that an energy of  $1.2 \pm 0.1$  eV is associated with the annealing of the displacement damage. Electron photoinjection experiments on the annealed samples indicate that both bleaching of the electron traps and annealing of the displacement damage is occurring during the thermal treatment.

#### d. Scanning Electron Microscope Studies

Some MOS capacitors have been examined using the electron beam of a scanning electron microscope as a radiation source. By controlling the energy of the incident electron beam it is possible to create electron/hole



pairs at various depths within the oxide. The samples were mounted in such a way that capacitance-voltage and conductance-voltage measurements could be made in the microscope. In this series of measurements the sample was exposed to a predetermined number of electrons ( $9 \times 10^{13}/\text{cm}^2$ ) at a given energy and then the flat band voltage and conductance measurements were made to determine the oxide charge storage and the density of interface states<sup>(8)</sup>. The electron beam energy was then increased in 100 volt steps and the procedure repeated until the beam penetrated through the oxide to the silicon. The gate electrode was grounded during these irradiations and the bias on the oxide was controlled by altering the potential of the silicon substrate. Preliminary results, obtained with implanted and unimplanted samples having 200 Å semitransparent gold gate electrodes, are shown in Fig. 5. The substrate bias of -10 volts during the irradiation implies that electrons were attracted towards the gate electrode and holes to the Si/SiO<sub>2</sub> interface.

For the unimplanted sample, the flat band voltage was seen to increase linearly with electron beam energy until the beam penetrated the gold electrode and deposited energy directly in the SiO<sub>2</sub>.

At this point the flat band voltage remained at the same value independent of beam energy. The implanted sample had an initially negative flat band voltage that corresponded to about 10% of the charge introduced into the oxide by the Al<sup>+</sup> ions. While the electron beam lost all of its energy in the gold gate electrode there was essentially no change in the flat band voltage. Once the beam penetrated to the SiO<sub>2</sub> negative charge was stored in the oxide, the initial positive charge being largely annihilated or compensated for by the time the beam penetrated to the Si/SiO<sub>2</sub> interface.

Because of the strong interaction between the electron beam and the gold gate electrode, depth resolution was not high in these measurements and X-ray photons generated in the gold also played a role in the oxide charge storage and interface state generation processes.

Figure 6 shows the dependence of the interface state density on the energy of the incident electron beam. The total electron flux is the same for each data point. It is seen that with the electrons stopping in the gate electrode or within the displacement damage zone of the oxide, the number of interface

states remains constant at the pre-irradiation level. Once the beam starts to penetrate the relatively undamaged  $\text{SiO}_2$ , interface state generation begins. The rate of interface state generation seems to increase once the electron beam reaches the interface and penetrates the Si substrate.

#### DISCUSSION

The data presented above indicate that  $\text{Al}^+$  implantation has a considerable effect on the saturated flat band voltage shift produced when an MOS capacitor is exposed to ionizing radiation under positive gate bias conditions, but only a small effect when the same device is irradiated under a negative bias. The fact that the implantation process can cause a net negative charge storage in an unannealed oxide at room temperature and that the trap levels associated with this charge storage anneal in the same temperature range in which optical, and E.S.R. absorption peaks associated with the implantation process also anneal<sup>(9)</sup>, suggests that the electron traps are associated with the displacement damage created during implantation, rather than with chemical effects due to the addition of  $\text{Al}^+$  ions to the matrix. This contention is supported by similar observations made by Emms et al.<sup>(10)</sup> where the implantation associated oxide modifications were found to be essentially independent of the implanting ion type. The data also suggest that the saturated flat band voltage shift is determined by that amount of charge which has to be stored in the oxide to reduce the bulk field to zero during X-irradiation, rather than on the number of new traps introduced during implantation. This follows from the relative independence of  $V(\text{sat})$  under positive gate bias conditions on the total number of implanted ions, a condition that obtains both before and after thermal annealing of these samples. The spatial distribution of these traps is important in determining the value of  $V(\text{sat})$  at a given gate bias as was indicated in Table I. It is also apparent that the major effect of the implantation is to provide compensatory electron traps in the oxide rather than providing electron/hole recombination paths. This is indicated by those experiments in which electrons were photodepopulated from the implantation associated traps by illuminating with 4.9 eV light under negative gate bias and the absence of a similar response in the unimplanted sample. This inter-

pretation is supported by the low temperature data on the unannealed sample where the additional hole traps in the  $\text{SiO}_2/\text{Si}$  interface region that become stable at  $80^\circ\text{K}$ <sup>(6)</sup> more than counteracted the electrons trapped in the bulk displacement damage zone and produced a negative flat band voltage shift. Holes in these traps could then be removed by photodepopulation and the flat band voltage made to change sign.

The qualitative features of charge storage in the implanted oxide under both positive and negative gate bias are understandable in terms of a simple model in which it is assumed that the major effect of a shallow  $\text{Al}^+$  implantation is to produce a zone of displacement damage within the oxide that can trap a high density of electrons and holes. As indicated schematically in Fig. 7, the unimplanted oxide is assumed to be essentially free of electron traps<sup>(11)</sup> and to have hole traps largely concentrated in the interface regions at the gate and silicon electrodes<sup>(12)</sup>. In the implanted oxide the hole traps at the  $\text{Si}/\text{SiO}_2$  interface are assumed to be similar in number to those in the unimplanted oxide and additional hole and electron traps are associated with the displacement damage zone generated by the implantation. This approximation may not be completely correct if the ionization produced during the implantation process creates new hole traps at the interface.

When the oxides are exposed to X-rays it is assumed that electron-hole pairs are generated uniformly throughout the oxide. Electron injection from the Si is ignored. In the displacement damage zone these carriers are expected to have a short mean free path before trapping in fields on the order of those encountered in device applications and would, therefore, charge compensate each other or recombine. In the relatively undamaged zone of the oxide, between the tail of the implantation profile and the silicon interface, both electrons and holes are assumed to be mobile and those which escape geminate recombination will move under the influence of the local field. It is assumed that the number of free electrons and holes depends linearly<sup>(13)</sup> upon the oxide field for fields below circa  $10^6$  volts  $\text{cm}^{-1}$ . On the basis of the data of Powell and Debenwick<sup>(12)</sup> and Srour et al.<sup>(13)</sup> it is assumed that electrons are not trapped at the  $\text{Si}/\text{SiO}_2$  interface but that some fraction,  $c$ , of the incident holes is trapped at this interface. Typically  $c$  has a value

of 10 → 15%. Electrons or holes incident on the radiation damage zone of the oxide are assumed to be completely trapped in a region extending from  $x = a$  to  $x = (a+b)$ , where  $x$  is measured from the metal insulator interface. This zone of the oxide will, therefore, have a net positive or negative charge at the end of a radiation exposure depending upon the sign of the gate voltage applied during irradiation. In the unannealed oxide there are assumed to be more traps in this damage region than are occupied by electrons or holes in the saturated flat band condition (when the field across the unimplanted region of the oxide has been reduced to zero by the trapped charges at its boundaries).

Under positive gate voltage conditions the numbers of trapped holes and electrons on the basis of this model are given by

$$\int_a^{a+b} N^- dx = \int_0^t J_e dt$$

and

$$\int_{x_0-d}^{x_0} P^+ dx = C \int_0^t J_h dt \quad (1)$$

where  $N^-$  and  $P^+$  are the density of trapped electrons and holes at the end of a radiation exposure of duration,  $t$ .  $J_e$  and  $J_h$  are the electron and hole fluxes and the quantities  $a$ ,  $b$ ,  $x_0$  and  $d$  are as defined in Figure 7. For this gate bias the electrons are trapped in the displacement damage zone and the holes at the Si/SiO<sub>2</sub> interface.

The electron and hole fluxes are linearly dependent upon the field in the undamaged part of the oxide and:

$$J_e = J_h = AE(x = a+b) \quad (2)$$

where A is a constant depending upon the carrier generation rate and the geminate recombination parameters and:

$$E(x=a+b) = \left( \frac{V_g}{x_0} \right) - \left( \frac{p^+}{\epsilon} \frac{d^2}{2x_0} \right) - \left( \frac{N^-}{\epsilon} \frac{(2ab + b^2)}{2x_0} \right) \quad (3)$$

where  $\epsilon$  is the dielectric constant of the  $\text{SiO}_2$ . Using these relationships, expressions may be developed for the rate of filling of electron and hole traps. These have the form

$$\frac{dP^+}{dt} = \frac{cA}{d} \left( \frac{V_g}{x_0} - \frac{1}{2\epsilon x_0} [P^+ d^2 + N^-(2ab+b^2)] \right) \quad (4)$$

and

$$\left( \frac{dN^-}{dt} \right) = \left( \frac{d}{bc} \right) \left( \frac{dP^+}{dt} \right)$$

The flat band voltage as a function of radiation time is then given by:

$$V_{FB} = - \frac{1}{\epsilon} \int_{x_0-d}^{x_0} x P^+(t) dx + \frac{1}{\epsilon} \int_a^{a+b} x N^-(t) dx \quad (6)$$

and substituting for  $P^+(t)$  and  $N^-(t)$  obtained from equations (4) and (5) using Laplace transform techniques and evaluating the integrals of Eq. (6) gives

$$V_{FB} = V_g \left[ 1 - \frac{2x_0 c}{cd + (2a+b)} \right] \left( 1 - \exp\left\{ -\frac{Bt}{x_0} \right\} \right) \quad (7)$$

where B is a constant for given radiation conditions. As  $t \rightarrow \infty$ ,  $V_{FB} \rightarrow V(\text{sat})$  and so

$$V(\text{sat}) = V_g \left[ 1 - \frac{2x_0 c}{cd + (2a+b)} \right] \quad (8)$$

The values of  $a$  and  $b$  are dependent upon the energy of the implanting ions. In order to compare the predictions of this model with the data obtained at different implantation energies,  $a$  and  $b$  have been related to numerical data <sup>(14)</sup> on the projected range,  $R$ , and standard deviation,  $\sigma$ , of the implantation profile. Using  $a = (R - 2\sigma)$  and  $b = 4\sigma$  the expression for  $V(\text{sat})$  can be simplified to give

$$V(\text{sat}) = V_g \left[ 1 - \frac{2x_o c}{cd + 2R} \right] \quad (9)$$

Using  $x_o = 1315 \text{ \AA}$ ,  $d = 300 \text{ \AA}$ ,  $c = 0.1$  and  $V_g = 10$  volts,  $V(\text{sat})$  can be computed for various implantation energies. These values are shown in Table I together with the projected range and standard deviation of the implantation profile. Considering the simplicity of the model the agreement with experiment is surprisingly good. Eq. (9) also indicates that there is an optimum projected range for producing a hard oxide when sufficient electron traps are available. For  $V(\text{sat}) = 0$

$$R = c(x_o - d/2) \quad (10)$$

Under negative gate bias all those electrons escaping geminate recombination will enter the silicon as it has been assumed that the undamaged oxide has no electron traps. The holes will be trapped in the trailing edge of the displacement damage zone between  $a$  and  $a+b$ . Carrier separation will continue until the field in the undamaged region of the oxide goes to zero because of the trapped hole charge. For this case:

$$\int_a^{a+b} P^+ dx = \int_0^t J_h dt \quad (11)$$

also  $J_h = J_e = AE$  where

$$E = \frac{V_g}{x_o} + \frac{P^+}{\epsilon} \frac{(2ab + b^2)}{2x_o} \quad (12)$$

and the final number of trapped holes is given by

$$p^+ = \frac{-2eV_g}{(2ab+b^2)} \quad (13)$$

under which condition  $V(\text{sat}) = V_g$  and oxide hardening is not possible. Again the prediction of the model is in reasonable agreement with experiment. Any electron trapping within the oxide, such as may occur at low temperatures, would be expected to make  $V(\text{sat})$  under negative gate voltage conditions less negative.

The thermal annealing experiments indicate that the implantation associated displacement damage anneals with an activation energy of  $1.2 \pm 0.1$  eV. The thermal depth of electron traps induced in  $\text{SiO}_2$  by implantation with Au ions has been determined by Chen et al.<sup>(15)</sup> to be essentially the same value. If these electron traps are associated with displacement damage, as is suggested by the present experiments, then both bleaching of the electron traps and their annealing by lattice recombination processes will occur in the same temperature range. The electron photoinjection experiments indicate that this is the case.

The flat band voltage behavior of the samples examined in the S.E.M. also indicates that the implant zone of the oxide is a source of traps for both electrons and holes. Electron-hole pairs generated by the electron beam stopping in this region either recombine or are trapped in approximately equal numbers. Once the electron beam penetrates beyond this region of high trap density those electron-hole pairs generated in the relatively undamaged region of the oxide may be separated by the applied field. A fraction of the holes incident upon the  $\text{SiO}_2/\text{Si}$  interface is trapped and create interface states. The electrons incident upon the damage zone are largely trapped and serve to charge compensate the holes at the  $\text{Si}/\text{SiO}_2$  interface.

The creation of interface states by the hole flux is suggested by the data of Fig. 6. In the implanted sample the number of these states remains relatively constant until the electron beam penetrates beyond the maximum of the implantation damage region. Hole transport to the  $\text{SiO}_2/\text{Si}$  interface can then occur and the interface state density increases with increasing

electron beam irradiation. In the unimplanted sample, where holes are assumed to be essentially free wherever they are generated, the number of interface states increases linearly with electron beam penetration into the oxide and remains approximately constant once the beam has penetrated to the  $\text{SiO}_2/\text{Si}$  interface.

Charge coupled devices are of interest for use as imaging systems in an "integrated focal plane". Killiany et al.<sup>(16)</sup> have shown that considerable image degradation may occur when such CCD's are exposed to as little as  $10^4$  rads. These authors suggest that standard MOS hardening techniques can be used to make a substantial improvement in the device hardness to ionizing radiation. The present measurements indicate that while this may be true at room temperature, devices cooled to low temperatures to increase their photon detection sensitivity cannot be satisfactorily radiation hardened by the same implantation technology that increases device radiation resistance at room temperature. Thermally stimulated current data indicates that the additional hole traps responsible for the low temperature oxide "softness" become unstable at circa 150K. Some cooling of the CCD structure should therefore be possible before these traps contribute to the device radiation sensitivity.



# REFERENCES

1. K. M. Schlesier, IEEE Trans. NS21 152 (1974).
2. K. G. Aubuchon, IEEE Trans. NS-18 117 (1971).
3. H. L. Hughes, R. D. Baxter and B. Phillips, IEEE Trans. NS-19 256 (1972).
4. E. Harari and B.S.H. Royce, IEEE Trans. NS-20 280 (1973).
5. K. H. Zaininger and E. P. Heiman, Solid State Technology 13, 49 May 1970.
6. E. Harari, S. T. Wang and B.S.H. Royce, J. Appl. Phys. 46, 1310 (1975).
7. E. Harari, Ph.D. thesis. Princeton University 1973.
8. E. H. Nicollian, A. Geotzberger and A. D. Lopez, Solid State Communications 12 937 (1969).
9. B.S.H. Royce, T. H. Russell, T. Pandolfi and E. Harari, Proc. Int. Color Center Conference, Sendai, Japan (1974), p. 181.
10. C.G. Emms, A. G. Holmes-Siedle, I. Groombridge and J. R. Bosnell, IEEE Trans. NS-21 159 (1974).
11. N. M. Johnson, W. C. Johnson and M. A. Lampert, J. Appl. Phys. 46, 1216 (1975).
12. R. Powell and G. Derbenwick, IEEE Trans. NS-18 99 (1971).
13. J. R. Srour, O. L. Curtis and K. Y. Chiu, IEEE Trans. NS-21 73 (1974).
14. R. G. Wilson and G. R. Brewer, "Ion Beams" Wiley (1973).
15. L. I. Chen, K. A. Pickar and S. M. Sze, Solid State Electronics 15 (1972) 979.

TABLE 1.

Implantation Energy (KeV)	10	20	30
Fluence. (cm <sup>-2</sup> )	10 <sup>15</sup>	10 <sup>14</sup>	10 <sup>15</sup>
V(sat) exptl. (volts)	3.0	5.5	7.0
R. (Å)	140	270	400
σ (Å)	45	80	110
V(sat) theor. volts	1.5	5.4	6.9

A comparison between the calculated and experimental  
saturated flat band voltages for implanted MOS capacitors.

#### FIGURE CAPTIONS

- Fig. 1. Saturated flat band voltage as a function of gate voltage during X-irradiation for an unimplanted sample.
- Fig. 2. Saturated flat band voltage as a function of gate voltage during X-irradiation for an implanted sample ( $10^{14}$  Al  $\text{cm}^{-2}$ ; 20 KeV).
- Fig. 3. Photodepopulation of trapped electrons in an unannealed sample following room temperature X-irradiation under positive bias. ( $10^{15}$  Al  $\text{cm}^{-2}$ ; 30 KeV).
- Fig. 4. Saturated flat band voltage measured at room temperature as a function of the annealing temperature of an implanted sample.
- Fig. 5. Flat band voltages of MOS capacitors as a function of electron beam energy for unimplanted and implanted samples.
- Fig. 6. Interface state generation as a function of electron beam energy in implanted and unimplanted samples.
- Fig. 7. Models for electron and hole trapping in unimplanted  $\text{SiO}_2$  MOS structures.

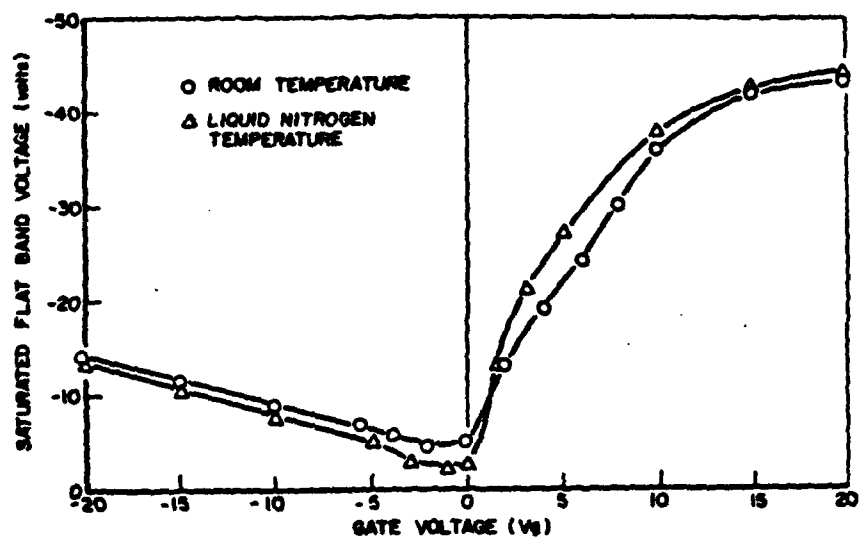


Figure 1

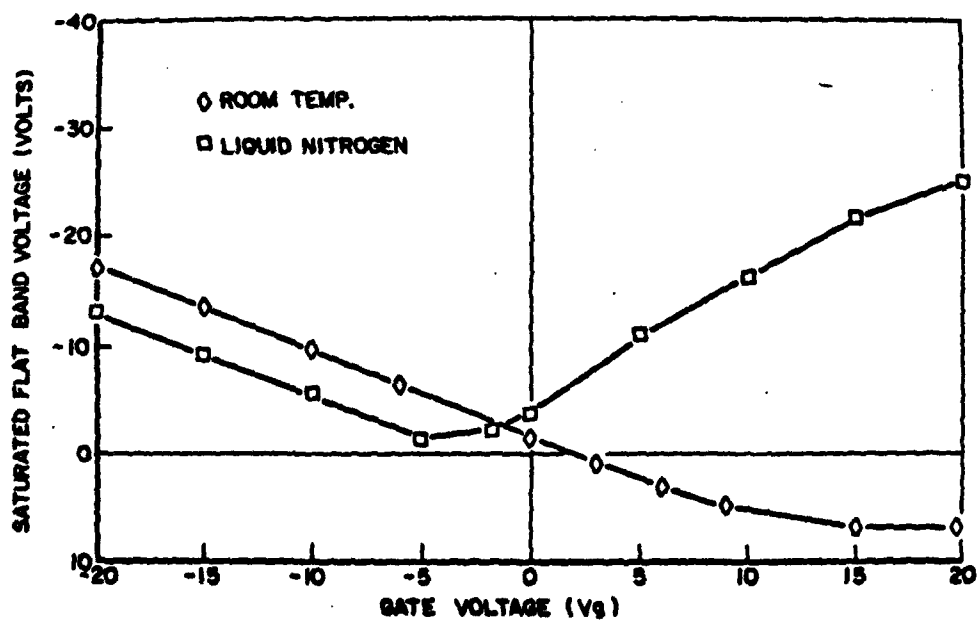


Figure 2

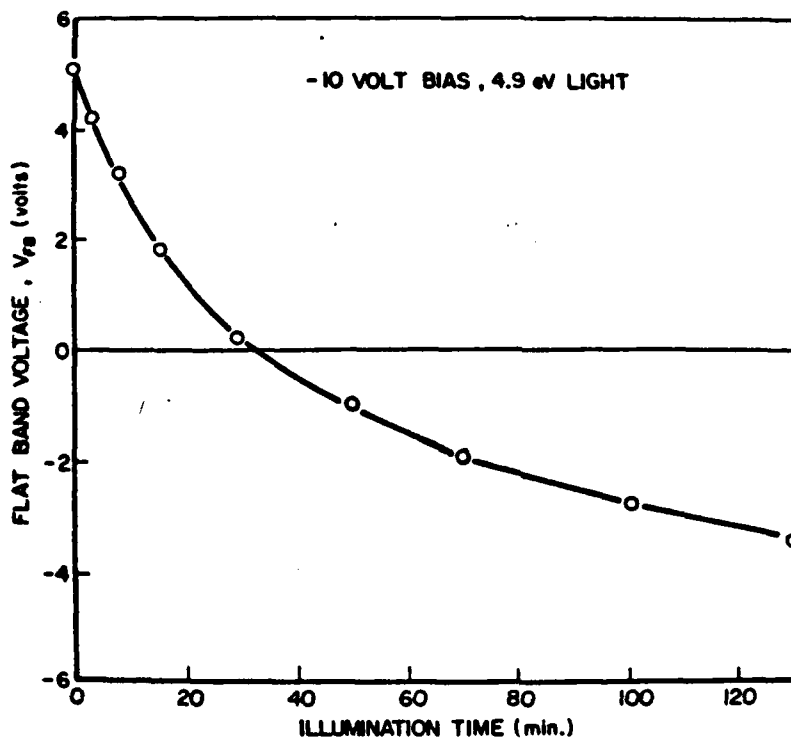
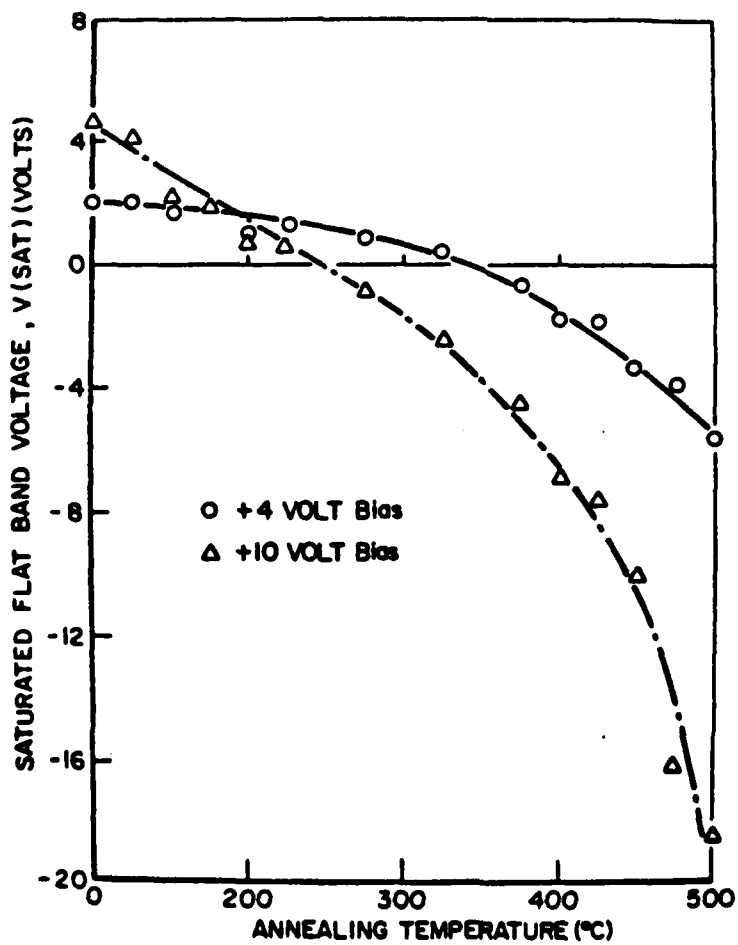


Figure 3



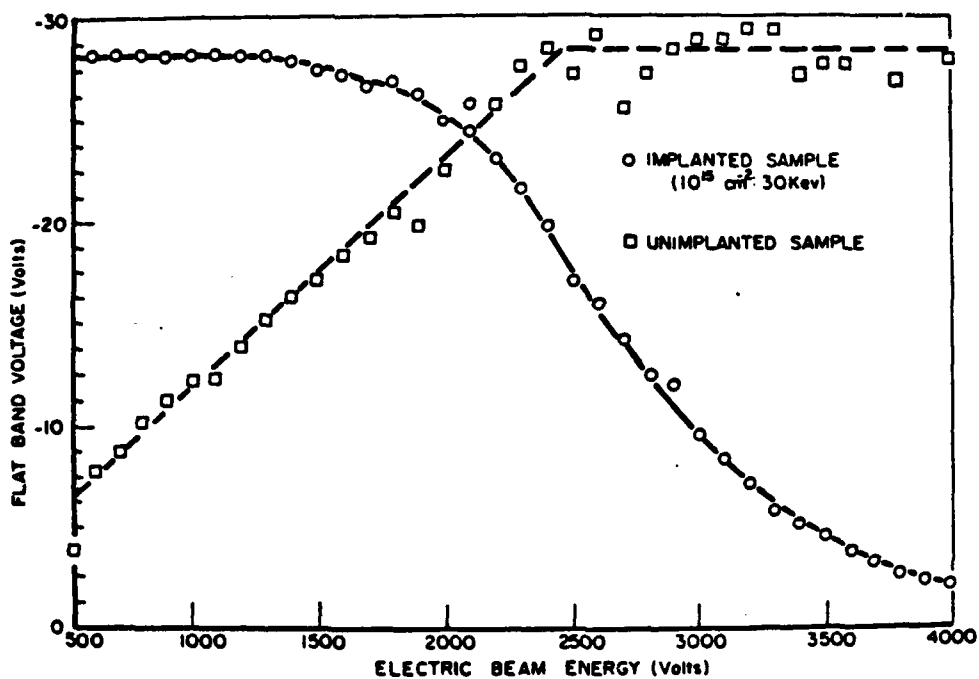


Figure 5

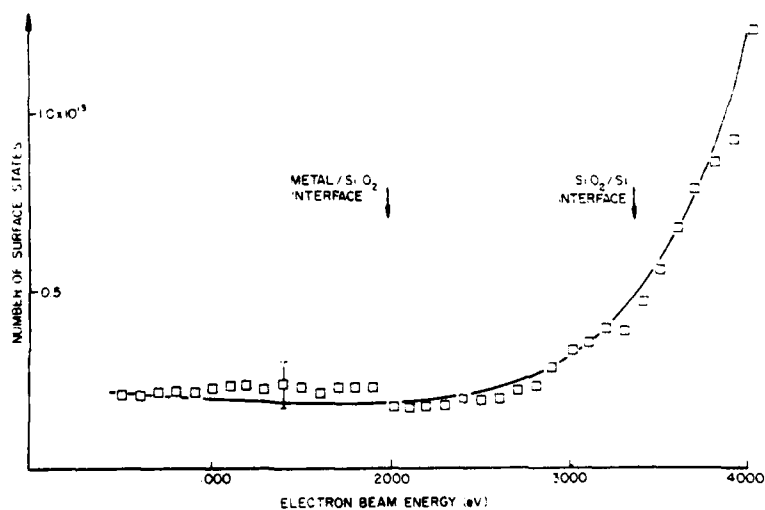


Figure 6

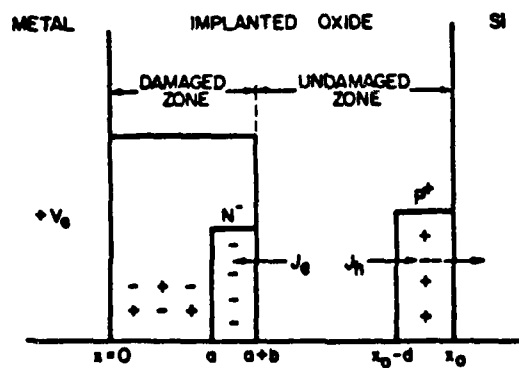
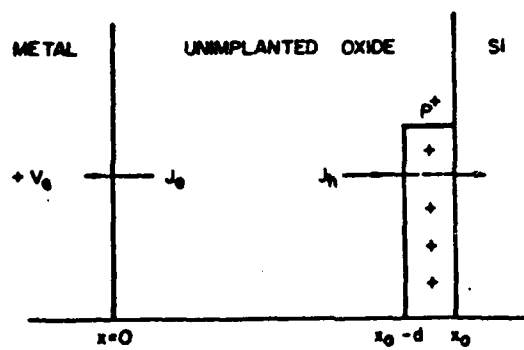


Figure 7

## DISTRIBUTION

### DEPARTMENT OF DEFENSE

Director  
Armed Forces Radiobiology  
Research Institute  
Defense Nuclear Agency  
National Naval Medical Center  
Bethesda, MD 20014  
Attn: Robert E. Carter

Defense Documentation Center  
Cameron Station  
Alexandria, VA 22314  
Attn: TC (12)

Director  
Defense Intelligence Agency  
Washington, DC 20301  
Attn: DS-4A2

Director  
Defense Nuclear Agency  
Washington, DC 20305  
Attn: STTL Tech. Library (2)  
DDST  
RATN  
RAEV

Commander  
Field Command  
Defense Nuclear Agency  
Kirtland AFB, NM 87115  
Attn: FCPR

Chief  
Livermore Div. Field Cmd., DNA  
Lawrence Livermore Laboratory  
P.O. Box 808  
Livermore, CA 94550  
Attn: Doc. Control for L-395

Director  
National Security Agency  
Ft. George G. Meade, MD 20755  
Attn: TDL  
O. O. van Gunten, R-425

Weapons Systems Evaluation Group  
400 Army-Navy Drive  
Arlington, VA 22202  
Attn: Document Control

Advisory Group on Electronic Devices  
201 Varnick Street, Ninth Floor  
New York, NY 10014  
Attn: Working Group B

### DEPARTMENT OF THE ARMY

Commander  
Frankford Arsenal  
Bridge & Tacony Streets  
Philadelphia, PA 19137  
Attn: SARFA-FCE, Marvin Elnick

Commander  
Harry Diamond Laboratories  
2800 Powder Mill Road  
Adelphia, MD 20783  
Attn: AMXDO-RBH, P. A. Caldwell  
AMXDO-RBI, J. A. Rosado  
AMXDO-RCC J. E. Thompson  
DRXDO-RT, R. J. Bostak  
DRXDO-TF, E. E. Conrad  
DRXDO-RBG, J. M. McGarrity

Commander  
Picatinny Arsenal  
Dover, NJ 07801  
Attn: SARPA-ND-N  
SARPA-ND-C-E, A. Nordio  
SMUPA-ND-W  
SMUPA-TN, B. Franks  
SARPA-FR-E, L. Avrami

Director  
U.S. Army Ballistic Research Labs  
Aberdeen Proving Ground, MD 21005  
Attn: AMXRD-BVL, D. Rigotti  
AMXBR-AM, W. van Antwerp  
AMXBR-X, J. Meszaros

Commander  
U.S. Army Electronics Command  
Fort Monmouth, NJ 07703  
Attn: AMSEL-CT-HDK, A. Cohen  
AMSEL-TL-IR, E. Hunter  
AMSEL-GG-TD, W. Werk  
AMSEL-TL-EN, R. Lux  
AMSEL-TL-MD, G. Gaule  
AMSEL-TL-ND, S. Kronenbey  
AMSEL-TL-EN, E. Both



Commander  
U.S. Army Missile Command  
Redstone Arsenal  
Huntsville, AL 35809  
Attn: AMCPM-LCEX, H. Henriksen  
AMSMI-RGP, H. Green  
AMSMI-RRR, F. Gibson

Commander  
U.S. Army Mobility Equip. R&D Ctr.  
Fort Belvoir, VA 22060  
Attn: STSFB-MW, J. Bond

Chief  
U.S. Army Nuc. & Chemical Surety Gp.  
Bldg. 2073, North Area  
Fort Belvoir, VA 22060  
Attn: MOSG-ND, Major S. Winslow

Commander  
U.S. Army Nuclear Agency  
Fort Bliss, TX 79916  
Attn: ATCN-W, LTC L. Sluga

Project Manager  
U.S. Army Tactical Data Systems, AMC  
Fort Monmouth, NJ 07703  
Attn: D. B. Huewe  
AMCPN-TDS-SD

Commander  
U.S. Army Test & Evaluation Cmd.  
Aberdeen Proving Ground, MD 21005  
Attn: AMSTE-NB, R. Galasso

#### DEPARTMENT OF THE NAVY

Chief of Naval Research  
Arlington, VA 22217  
Attn: Code 421, D. Padgett  
Code 427

Commanding Officer  
Naval Ammunition Depot  
Crane, IN 47522  
Attn: Code 7024, J. Ramsey  
Code 70242, J. Munarin

Commander  
Naval Electronic Systems Command  
Washington, DC 20360  
Attn: Code 504510  
ELEX 05323, C. Watkins  
PME 117-21

Commanding Officer  
Naval Intelligence Support Ctr.  
4301 Suitland Road, Bldg. 5  
Washington, DC 20390  
Attn: P. Alexander

Director  
Naval Research Laboratory  
Washington, DC 20375  
Attn: Code 4004, E. Brancato  
Code 5210, J. Davey  
Code 7701, J. Brown  
Code 6460, D. Mitchell  
Code 6631, J. Ritter  
Code 5216, H. Hughes  
Code 2627, D. Folen

Commander  
Naval Sea Systems Command  
Washington, DC 20362  
Attn: SEA-9931, R. Lane

Commander  
Naval Surface Weapons Center  
Dahlgren, VA 22448  
Attn: W. H. Holt

Commanding Officer  
Nuclear Weapons Center Pacific  
Naval Air Station, North Island  
San Diego, CA 92135  
Attn: Code 50

Commander  
Naval Surface Weapons Center  
Silver Spring, MD 20910  
Attn: F. E. Warnock  
R. A. Smith  
M. C. Petree

DEPARTMENT OF THE AIR FORCE

AF Cambridge Research Labs  
L. G. Hanscom Field, MA 01730  
Attn: LQR, E. A. Burke  
J. E. Cormier  
B. Buchanan  
D. Neaman

AF Materials Laboratory  
Wright-Patterson AFB, OH 45433  
Attn: LTE

AF Weapons Laboratory  
Kirtland AFB, NM 87117  
Attn: SAB  
J. S. Nichols

AFTAC  
Patrick AFB, FL 32925  
Attn: TAE

AF Avionics Laboratory  
Wright-Patterson AFB, OH 45433  
Attn: AFAL-TEA, H. Hennecke

Space & Missile Systems Organization  
P.O. Box 92960, Worldway Postal Ctr.  
Los Angeles, CA 90009  
Attn: DYS, Major L. Darda  
DYS, Capt. W. Schober  
SZJ, Capt. J. Salch  
YDD, Maj. M. Schneider

Space & Missile Systems Organization  
Norton AFB, CA 92409  
Attn: MNNG, Capt. D. Strobel

Commander in Chief  
Strategic Air Command  
Offutt AFB, NM 68113  
Attn: XPFS, Maj. B. Stephan

USERDA

University of California  
Lawrence Livermore Laboratory  
P.O. Box 808  
Livermore, CA 94550  
Attn: R. L. Ott, L-531  
L. Cleland, L-156  
F. Kovar, L-94  
D. J. Meeker, L- 53

Los Alamos Scientific Laboratory  
P.O. Box 1663  
Los Alamos, NM 87545  
Attn: B. W. Noel  
J. A. Freed  
M. M. Hoffman

Sandia Laboratories  
Livermore Laboratory  
P.O. Box 969  
Livermore, CA 94550  
Attn: T. A. Dellin

Sandia Laboratories  
P.O. Box 5800  
Albuquerque, NM 87115  
Attn: C. J. MacCallum  
J. V. Walker, 5220  
Org. 1933, F. N. Coppage  
H. Sander  
B. L. Gregory

U.S. Energy Research & Dev. Admin.  
Albuquerque Operations Office  
P.O. Box 5400  
Albuquerque, NM 87115  
Attn: WSSB

OTHER GOVERNMENT AGENCIES

Central Intelligence Agency  
Washington, DC 20505  
Attn: RD/SI, Alice A. Padgett

Department of Commerce  
National Bureau of Standards  
Washington, DC 20234  
Attn: J. C. French  
R. Placidus, Appl. Rad. Div.  
K. F. Galloway  
M. G. Buehler

DoD CONTRACTORS

Aerojet ElectroSystems Co.  
P.O. Box 296  
Azusa, CA 91702  
Attn: T. D. Hanscome

Aeronutronic Ford Corporation  
Ford & Jamboree Roads  
Newport Beach, CA 92663  
Attn: K. C. Attinger  
Tech. Info. Section

Aeronutronic Ford Corporation  
3939 Fabian Way  
Palo Alto, CA 94303  
Attn: S. R. Crawford, MS 531  
D. R. McMorrow, MS G30

Aerospace Corporation  
P.O. Box 92957  
Los Angeles, CA 90009  
Attn: I. M. Garfunkel  
W. W. Willis  
M. J. Bernstein  
Julian Reinheimer  
L. W. Aukerman  
Library

Avco Research & Systems Group  
201 Lowell Street  
Wilmington, MA 01887  
Attn: Research Lib., A830

BDM Corporation  
P.O. Box 9274  
Albuquerque, NM 87119  
Attn: T. H. Neighbors

Bell Aerospace Company  
P.O. Box 1  
Buffalo, NY 14240  
Attn: C. B. Schoch

Bendix Corporation  
Communication Division  
East Joppa Road - Towson  
Baltimore, MD 21204  
Attn: Document Control

Bendix Corporation  
Southfield, MI 48076  
Attn: D. J. Niehaus, Prog. Devel.

Boeing Company  
P.O. Box 3707  
Seattle, WA 98124  
Attn: D. L. Dye, MS 87-75  
H. W. Wicklein, MS 17-11  
R. S. Caldwell, 2R-00  
Aerospace Library

Booz-Allen & Hamilton, Inc.  
106 Apple Street  
New Shrewsbury, NJ 07724  
Attn: R. J. Chrisner

Charles Stark Draper Lab, Inc.  
68 Albany Street  
Cambridge, MA 02139  
Attn: P. R. Kelly  
R. G. Haltmaier  
K. Fertig

Computer Sciences Corporation  
201 La Veta Drive, NE  
Albuquerque, NM 87108  
Attn: R. H. Dickhaut

Cutler-Hammer, Inc.  
AIL Division  
Comac Road  
Deer Park, NY 11729  
Attn: A. Anthony

Dikewood Corporation  
1009 Bradbury Drive, SE  
Albuquerque, NM 87106  
Attn: L. W. Davis

E-Systems, Inc.  
Greenville Division  
P.O. Box 1056  
Greenville, TX 75401  
Attn: Library, 8-50100

Effects Technology, Inc.  
5383 Holister Avenue  
Santa Barbara, CA 93105  
Attn: E. J. Steele

Exp & Math Physics Consultants  
P.O. Box 66331  
Los Angeles, CA 90066  
Attn: T. M. Jordan

Fairchild Camera & Instr. Corp.  
464 Ellis Street  
Mountain View, CA 94040  
Attn: D. K. Myers

Fairchild Industries, Inc.  
20301 Century Blvd.  
Germantown, MD 20767  
Attn: Mgr. Config. Data & Stds.

Franklin Institute  
20th St. & Parkway  
Philadelphia, PA 19103  
Attn: R. H. Thompson

General Electric Company  
Space Division  
P.O. Box 8555  
Philadelphia, PA 19101  
Attn: L. I. Chasen  
J. P. Spratt  
J. L. Andrews  
J. C. Peden, CCF 8301

General Electric Company  
Reentry & Envir. Systems Div.  
P.O. Box 7722  
Philadelphia, PA 19101  
Attn: Robert V. Benedict

General Electric Company  
TEMPO Center for Advanced Studies  
P.O. Drawer QQ  
Santa Barbara, CA 93102  
Attn: DASIAC  
M. Espig  
R. R. Rutherford

General Electric Company  
P.O. Box 1122  
Syracuse, NY 13201  
Attn: CSP 0-7, L. H. Dee

General Electric Company  
Aircraft Engine Group  
Evendale Plant  
Cincinnati, OH 45215  
Attn: J. A. Ellerhorst, E2

General Electric Company  
Aerospace Electronics Systems  
Utica, NY 13503  
Attn: W. J. Patterson, Drop 233

General Electric Company  
P.O. Box 5000  
Binghamton, NY 13902  
Attn: D. W. Pepin, Drop 160

General Electric Company/DASIAC  
c/o Defense Nuclear Agency  
6801 Telegraph Road  
Alexandria, VA 22310  
Attn: William Alfonte

General Research Corporation  
P.O. Box 3587  
Santa Barbara, CA 93105  
Attn: R. D. Hill

GTE Sylvania, Inc.  
77 A Street  
Needham, MA 02194  
Attn: C. A. Thornhill  
J. A. Waldon  
L. L. Blaisdell

GTE Sylvania, Inc.  
189 B Street  
Needham Heights, MA 02194  
Attn: H. A. Ullman  
P. B. Fredrickson  
C. H. Ramsbottom

Harris Corporation, Semicon. Div.  
P.O. Box 883  
Melbourne, FL 32901  
Attn: W. E. Abare, MS 16-111  
C. F. Davis, MS 17-220  
T. L. Clar, MS 4040

Hazeltine Corporation  
Pulaski Road  
Green Lawn, NY 11740  
Attn: Tech. Info. Ctr.

Honeywell, Inc.  
2600 Ridgeway Parkway  
Minneapolis, MN 55413  
Attn: R. R. Johnson, A1622

Honeywell, Inc.  
13350 U.S. Highway 19  
St. Petersburg, FL 33733  
Attn: S. H. Graff, MS 725-J

Honeywell, Inc.  
2 Forbes Road  
Lexington, MA 02173  
Attn: Technical Library

Hughes Aircraft Company  
Centinela and Teale  
Culver City, CA 90230  
Attn: Dan Binder, MS 6-D147  
B. W. Campbell, MS 6-E110  
K. R. Walker, MS D157

Hughes Aircraft Company  
Space Systems Division  
P.O. Box 92919  
Los Angeles, CA 90009  
Attn: E. C. Smith, MS A620  
W. W. Scott, MS A1080

Hughes Aircraft Company  
500 Superior Avenue  
Newport Beach, CA 92663  
Attn: K. G. Aubuchon  
E. Harari

IBM Corporation  
Route 17C  
Owego, NY 13827  
Attn: Frank Frankovsky

IRT Corporation  
P.O. Box 80187  
San Diego, CA 92138  
Attn: J. A. Naber  
T. M. Flanagan  
R. E. Leadon  
D. P. Snowden  
J. M. Wilkenfeld  
Library (2)

Ion Physics Corporation  
South Bedford Street  
Burlington, MA 01803  
Attn: Robert D. Evans

Kaman Sciences Corp.  
P.O. Box 7463  
Colorado Springs, CO 80933  
Attn: A. P. Bridges  
W. E. Ware  
D. H. Bryce

Litton Systems, Inc.  
5500 Canoga Avenue  
Woodland Hills, CA 91364  
Attn: Val J. Ashby, MS 67

Lockheed Missiles & Space Co.  
P.O. Box 504  
Sunnyvale, CA 94088  
Attn: E. Smith, Dept. 85-85  
P. J. Hart, Dept. 81-14  
G. F. Heath, Dept. 81-14  
B. T. Kimura, Dept. 81-14  
H. L. Schneemann, Dept. 81-64

LTV Aerospace Corp.  
P.O. Box 5907  
Dallas, TX 75222  
Attn: Technical Data Center

Martin-Marietta Aerospace  
P.O. Box 5837  
Orlando, FL 32805  
Attn: M. C. Griffith, MP-30  
W. W. Mras, MP-413

Martin-Marietta Corp.  
P.O. Box 179  
Denver, CO 80201  
Attn: Research Lib., 6617  
B. T. Graham, MS PO-454  
J. E. Goodwin, MS 0452

McDonnell Douglas Corp.  
P.O. Box 516  
St. Louis, MO 63166  
Attn: Technical Library

McDonnell Douglas Corp.  
5301 Bolsa Avenue  
Huntington Beach, CA 92647  
Attn: Stanley Schneider

Mission Research Corporation  
735 State Street  
Santa Barbara, CA 93101  
Attn: W. C. Hart

National Academy of Sciences  
Attn: National Materials Adv. Bd.  
2101 Constitution Avenue  
Washington, DC 20418  
Attn: R. S. Shane

University of New Mexico  
1821 Roma, NE  
Albuquerque, NM 87106  
Attn: W. W. Grannemann

Northrop Corporation  
1 Research Park  
Palos Verdes Peninsula, CA 90274  
Attn: V. R. DeMartino  
B. T. Ahlport  
G. H. Towner

Northrop Corporation  
3401 West Broadway  
Hawthorne, CA 90250  
Attn: D. N. Pocock  
J. Srouer

Physics International Company  
2700 Merced Street  
San Leandro, CA 94577  
Attn: C. H. Stallings  
J. H. Huntington

R&D Associates  
P.O. Box 9695  
Marine del Rey, CA 90291  
Attn: S. Clay Rogers

Raytheon Company  
Hartwell Road  
Bedford, MA 01730  
Attn: G. H. Joshi

RCA Corporation, Sarnoff Res. Ctr.  
P.O. Box 432  
Princeton, NJ 08540  
Attn: K. H. Zaininger  
R. J. Powell

Rensselaer Polytechnic Inst.  
P.O. Box 965  
Troy, NY 12181  
Attn: R. J. Gutmann

Research Triangle Institute  
P.O. Box 12194  
Research Triangle Park, NC 27709  
Attn: Eng. Div., M. Simons

Rockwell International Corp.  
3370 Miraloma Avenue  
Anaheim, CA 92803  
Attn: G. C. Messenger, FB61  
J. E. Bell, HA10  
D. J. Stevens, FA70

Rockwell International Corporation  
Collins Radio Group  
5225 C Avenue, NE  
Cedar Rapids, IA 52406  
Attn: Dennis Sutherland

Sanders Associates, Inc.  
95 Canal Street  
Nashua, NH 03060  
Attn: MDE, L. Aitel, NCA 1-3236

Science Applications, Inc.  
1651 Old Meadow Road  
McLean, VA 22101  
Attn: W. L. Chadsey

Science Applications, Inc.  
P.O. Box 2351  
La Jolla, CA 92038  
Attn: J. R. Beyster  
Larry Scott

Science Applications, Inc.  
2109 W. Clinton Avenue  
Huntsville, AL 35805  
Attn: N. R. Byrn

Science Applications, Inc.  
2680 Hanover Street  
Palo Alto, CA 94303  
Attn: Charles Stevens

Simulation Physics, Inc.  
41 B Street  
Burlington, MA 01803  
Attn: R. G. Little

Simulation Physics, Inc.  
17921-B Sky Park Blvd.  
Irvine, CA 92707  
Attn: A. J. Armini

Singer Company  
1150 McBride Avenue  
Little Falls, NJ 07424  
Attn: Irwin Boldman

Sperry Rand Corporation  
Systems Management Div.  
Great Neck, NY 11020  
Attn: C. L. Craig, EV  
P. Maraffino

Stanford Research Institute  
333 Ravenswood Avenue  
Menlo Park, CA 94025  
Attn: R. A. Armistead  
P. J. Dolan

Stanford Research Institute  
306 Wynn Drive, NW  
Huntsville, AL 35805  
Attn: MacPherson Morgan

Sundstrand Corporation  
4751 Harrison Avenue  
Rockford, IL 61101  
Attn: C. B. White

Texas Instruments, Inc.  
P.O. Box 5474  
Dallas, TX 75222  
Attn: G. F. Hanson  
D. J. Manus, MS 72  
S. B. Cox Jr., MS 909

TRW Semiconductors  
14520 Aviation Blvd.  
Lawndale, CA 90260  
Attn: R. N. Clarke

TRW Systems Group  
One Space Park  
Redondo Beach, CA 90278  
Attn: R. H. Kingsland, R1-2154  
W. H. Robinette Jr.  
P. Molmud, R1-1196  
J. I. Lubell  
R. D. Loveland, R1-1028  
A. A. Witteles, R1-1120  
L. D. Singletary, R1-1070  
A. H. Narevsky, R1-2144  
A. M. Liebschutz, R1-1162  
Allan Anderman, R1-1132

TRW Systems Group  
P.O. Box 1310  
San Bernardino, CA 92402  
Attn: E. W. Allen  
H. S. Jensen  
J. E. Dahnke

V. A. J. van Lint  
Mission Research Corporation  
7650 Convoy Court  
San Diego, CA 92111

Varian Associates  
611 Hansen Way  
Palo Alto, CA 94303  
Attn: D. C. Lawrence

Westinghouse Electric Corp.  
P.O. Box 1693  
Friendship International Airport  
Baltimore, MD 21203  
Attn: H. P. Kalapaca, MS 3525

Westinghouse Electric Corporation  
1310 Beulah Road,  
Pittsburgh, PA 15235  
Attn: W. E. Newell

Princeton University  
Dept. of Aerospace & Mech. Sci.  
Princeton, NJ 08540  
Attn: B. S. H. Royce